ISSN (Online) 2456-1290

International Journal of Engineering Research in Mechanical and Civil Engineering (IJERMCE)

Volume 12, Issue 10, October 2025

Development of a High Dimensional Precision Vacuum Die Casting System for Silicone and Polyurethane Components

[1] Veerendra Rajendrayya Swami, [2] Dr. Rajkumar G R, [3] Dr. Shanmukha Nagaraj, [4] Rohan R

[1] M.Tech., Scholar, Department of Mechanical Engineering, R V College of Engineering, Bengaluru, Karnataka, India
[2] Associate Professor, Department of Mechanical Engineering, R V College of Engineering, Bengaluru, Karnataka, India
[3] Associate Professor, Head of Mechanical Engineering Department, RV College of Engineering, Bengaluru, Karnataka, India
[4] Managing Director, Addere Creations, Bengaluru, Karnataka, India
Corresponding Author Email: [1] veerendrars.pdm23@rvce.edu.in, [2] rajkumargr@rvce.edu.in, [3] shanmukhan@rvce.edu.in, [4] rohanr@gmail.com

Abstract*— This research paper presents the design and computational validation of a high-dimensional vacuum die casting chamber intended for the production of high-precision silicone and polyurethane components. The chamber, measuring 610 mm x 680 mm x 1270 mm, was modeled and analyzed using CAD tools and ANSYS simulation environments. Emphasis was placed on structural integrity under atmospheric pressure, air evacuation dynamics, and effective vacuum maintenance. CFD and static structural simulations were conducted to assess pressure distribution, velocity profiles, and von Mises stress values. Results demonstrate the chamber's capability to reach vacuum conditions under 70 Torrs within 7 minutes and maintain the vacuum for up to two hours, validating its ability for elastomeric material casting. To validate the physical design and assess assembly feasibility, a scaled 3D-printed prototype of the vacuum die casting system was fabricated.

Keywords: Vacuum die casting, CFD simulation, structural analysis, silicone casting, polyurethane molding, ANSYS Fluent, vacuum chamber design.

I. INTRODUCTION

The casting of high-precision silicone and polyurethane components plays a critical role in modern manufacturing, particularly in the domains of automotive interiors, aerospace insulation, medical devices, consumer electronics, and industrial equipment.

These elastomeric materials are favored for their unique mechanical and chemical properties—ranging from flexibility, impact resistance, and thermal stability to excellent electrical insulation and biocompatibility.

In achieving flawless quality in these components—free from bubbles, shrinkage cavities, or dimensional inconsistencies—requires highly controlled casting environments. One of the most effective approaches to overcome these quality challenges is the use of vacuum-assisted die casting.

In vacuum casting, air and entrapped gases are eliminated from the mold cavity before and during the pouring of the material. For elastomeric materials like silicone and polyurethane, which tend to trap air due to their viscosity and curing characteristics, the vacuum process ensures smooth, void-free filling and minimizes the risk of internal porosity or surface defects. Moreover, many silicone and polyurethane formulations are sensitive to humidity and require moisture-free atmospheric conditions for proper curing and crosslinking. This makes vacuum casting not only advantageous but often essential in ensuring functional and visual integrity.

II. PROBLEM STATEMENT

To achieve the desired vacuum pressure and ensure efficient evacuation within an optimal time frame, the system must be designed with a high-performance vacuum pump, well-sealed chamber architecture, and minimal internal leakage paths. Proper sizing of the outlet ports, along with streamlined internal geometry, is essential to reduce flow resistance and enhance evacuation speed. Additionally, the use of pressure sensors and controlled valve mechanisms can enable precise regulation and monitoring of vacuum levels throughout the process. By optimizing these parameters, the system can consistently reach low vacuum pressures necessary for removing trapped air and moisture, ultimately resulting in improved material flow, reduced porosity, and high-quality casting of silicone and polyurethane components.

This research addresses the gap in design and simulation of such a system by developing a high-dimensional vacuum casting setup and conducting in-depth analysis—including structural and CFD studies—ensuring suitability for industrial-grade silicone and polyurethane component manufacturing.

ISSN (Online) 2456-1290

International Journal of Engineering Research in Mechanical and Civil Engineering (IJERMCE)

Volume 12, Issue 10, October 2025

III. LITERATURE REVIEW

1. Vacuum Chamber Design, Control, and Analysis

Vacuum chambers used in precision casting demand specialized materials, sealing mechanisms, and accurate vacuum regulation. Researchers have developed advanced materials with enhanced thermal and mechanical properties to improve chamber performance and durability [1]. Integration of smart sensors within the vacuum environment has enabled real-time monitoring of pressure and system behavior [2], while machine learning and AI models are increasingly used for automated control and predictive maintenance [3], [4]. IoT-based smart vacuum systems offer enhanced remote accessibility and monitoring [5]. Advanced leakage detection using deep learning and image recognition improves the reliability of vacuum systems [6], with conventional approaches also being effective for system diagnostics and repair [8]. High-precision leakage control and sealing enhancements ensure pressure stability during casting [9]. CFD-based thermal modeling has been employed to manage thermal gradients and insulation within the vacuum chambers [10], while hybrid vacuum pumps offer energy-efficient solutions [11]. Time-dependent vacuum simulations help in understanding evacuation behavior for process planning [12], and geometric modifications to chamber designs have shown improvements in evacuation rates and performance [13].

The integration of smart manufacturing principles is also transforming vacuum chamber operations. The adaptation of Industry 4.0 systems with data analytics, connectivity, and predictive algorithms has enabled real-time control and optimization [14]. High-speed evacuation models based on CFD simulations allow rapid vacuum generation [15], and robust sealing systems play a crucial role in maintaining vacuum integrity under cyclic thermal and mechanical stresses [16]. CFD simulations validated with experimental studies offer precise analysis of vacuum flow characteristics [17]. Transient pressure modeling supports accurate evacuation forecasting [18], while turbulence-enhanced CFD improves modeling precision [19]. Surface finish of chamber walls significantly affects leakage performance and must be carefully considered in manufacturing [20]. Heat transfer models assist in maintaining uniform temperature distribution during casting [21], and simulation-based chamber design ensures efficiency and reliability [22]. AI-powered optimization helps reduce evacuation times and energy use [23], and smart sensor networks facilitate real-time vacuum data acquisition [24]. Finally, digital twin systems create real-time virtual models of the chamber for predictive control and adaptive decision-making [25].

2. Die Casting System Design and Performance

Die casting processes demand precise thermal and flow control, especially for materials like silicone and polyurethane, which are sensitive to temperature and flow inconsistencies. Selecting advanced die materials improves dimensional accuracy and casting repeatability [26]. Adaptive control systems in vacuum die casting adjust casting parameters in real time to maintain consistent product quality, especially for high-precision applications [27]. Research into new die materials has revealed their benefits in resisting thermal deformation, improving surface quality, and prolonging tool life [28]. CFD-based evacuation analysis has played a significant role in understanding the airflow and pressure drop during mold evacuation, directly affecting defect reduction and mold filling [29]. Automation and smart control integration within die casting operations have contributed to better cycle control, minimizing manual errors and improving repeatability [30].

Material flow dynamics are central to vacuum-assisted die casting success. Computational analysis has been used to study flow behavior, aiding in the identification and mitigation of porosity, air entrapment, and incomplete filling [31]. Cycle optimization techniques that balance quality, cycle time, and thermal efficiency are essential for achieving high throughput without compromising casting integrity [32].

IV. METHODOLOGY

The methodology for developing the high-dimensional precision vacuum die casting system for silicone and polyurethane components began with an in-depth review of contemporary research on vacuum chambers, evacuation dynamics, and die casting technologies. Based on identified gaps, a conceptual CAD model of the vacuum chamber, die assembly, pouring system, and stirring mechanism was created using SolidWorks and ANSYS SpaceClaim. The chamber was dimensioned at approximately 1270 mm × 680 mm × 610 mm, designed with adequate provisions for vacuum sealing, sensor integration, and mold alignment. AISI 304 stainless steel was selected for the chamber due to its structural and thermal stability, while mold components used thermally conductive and non-stick materials compatible with silicone and polyurethane. Static structural analysis in ANSYS was conducted to evaluate stress and deformation due to external atmospheric pressure (~101325 Pa), verifying design integrity and seal reliability under vacuum conditions.

ISSN (Online) 2456-1290

International Journal of Engineering Research in Mechanical and Civil Engineering (IJERMCE)

Volume 12, Issue 10, October 2025

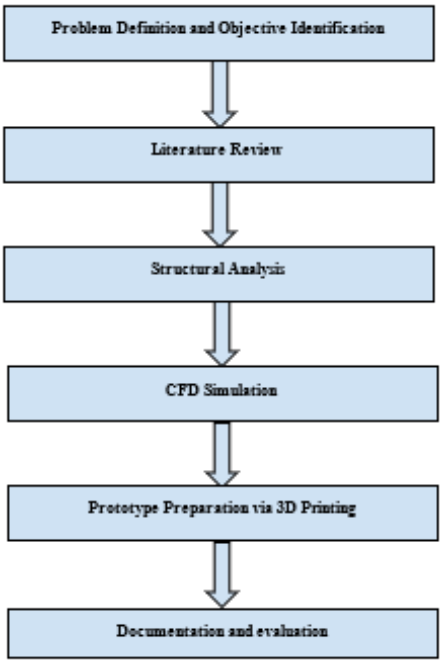

Fig 1: Methodology

Further, CFD simulations in ANSYS Fluent modeled evacuation dynamics under a **70 Torr vacuum (~9333 Pa)**, capturing air velocity, pressure gradients, and potential entrapment zones.

V. DESIGN CALCULATIONS

1. Geometric Vacuum Chamber

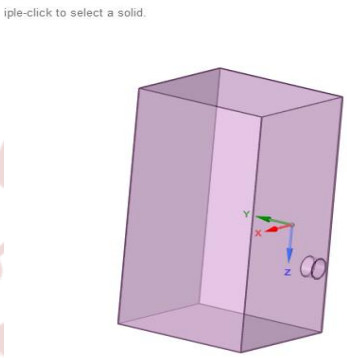

Fig 2: Vacuum Chamber

Length (L) = 610 mm, Width (W) = 680 mm,
Height (H) =1260 mm

2. Volume Calculation

V=L×W×H=1.27×0.61×0.68 = 0.472 m³

This volume is used for evacuation time and flow rate estimations.

3. Vacuum Evacuation Calculations

To achieve the desired vacuum performances the modelling of the pressure decay using isothermal assumptions and ideal gas behavior is carried out.

Ideal Gas Law Application

Under isothermal conditions (T = constant), the ideal gas law simplifies to:

$$\frac{P1}{P2} = \frac{n1}{n2}$$

For a control volume, the pressure decay with time during evacuation can be modeled using:

$$P(t) = P_0 . e^{-(\frac{S}{V})t}$$

Where:
P0 = Initial pressure (100,000 Pa)
P(t)= Pressure at time t
S = Pumping speed (m³/s)
V = Volume of chamber (0.472 m³)

Assuming a pump with a nominal capacity of 28 m³/h = 0.00778 m³/s, we calculate the time required to reach vacuum levels of 1000 Pa and 100 Pa.

Time to Reach Target Pressures

For P(t)=1000 Pa

$$\frac{1000}{100000} = e^{-(\frac{0.00778}{0.472})t} \Rightarrow ln(0.01) = -0.01649t \Rightarrow t = \frac{-4.605}{-0.01649} = 279 seconds$$

For P(t)=100Pa

$$\frac{100}{100000} = e^{-(\frac{0.00778}{0.472})t} \Rightarrow ln(0.001) = -0.01649t \Rightarrow t = \frac{-6.907}{-0.01649} = 419 seconds$$

This theoretical estimation is in close agreement with the results of ANSYS Fluent simulation, which showed vacuum levels reaching below 100 Pa in approximately 7 minutes.

4. Pump Power Sizing

Mass Flow Rate Calculations

During chamber evacuation, the air is displaced at a continuously reducing pressure. The flow regime is laminar viscous in most parts of the evacuation due to the relatively low Reynolds number.

Mass Flow Rate

Assuming air as an ideal gas:
$\dot{m}=\rho .Q$
$\dot{m}$ = 1.17×0.00778 = **0.0091kg/s**

At lower pressures, the mass flow rate reduces proportionally. The simulation data showed a flow rate decay from **~0.0091 kg/s to 10^{-7} kg/s** as vacuum was reached.

5. Structural Design Calculation

The chamber must withstand a maximum external pressure of atmospheric level (0.101 MPa), which acts uniformly on its surfaces.

ISSN (Online) 2456-1290

International Journal of Engineering Research in Mechanical and Civil Engineering (IJERMCE)

Volume 12, Issue 10, October 2025

External Pressure Load on Plates

For a rectangular plate under external pressure, the stress can be estimated using:

$$\sigma = \frac{0.3Pa^2}{t^2}$$

Assuming:
P = 0.101 MPa
Plate dimension a = 0.61 m
Wall thickness t = 10 mm

σ = 0.3 * 0.101 * 0.6120.012 = 113.06 MPa

The yield strength of stainless steel AISI 304 is ~215 MPa, so the factor of safety:

$$FOS = \frac{215}{113.06} = 1.9$$

This satisfies the safety margin and is supported by structural simulation results with a maximum stress of ~108 MPa.

Thermal Considerations for Polyurethane/Silicone Casting

Silicone and polyurethane often require curing temperatures ranging from 60°C to 150°C. The vacuum chamber and molds are designed to handle this thermal load without deformation or loss of sealing.

Thermal Expansion Check

Mild steel thermal expansion coefficient :
α=17×10-6/°C
For temperature rise of 100°C over 1 m length:
ΔL= α × L × ΔT=17×10-6×1×100 =1.7mm
Proper clearances and gasket designs are included to accommodate this expansion.

Gasket Compression and Sealing Calculations

Force for Gasket Compression

Assuming:
Gasket width = 5 mm
Compression = 20%
Gasket contact length = perimeter ≈ 4 × (1.27 + 0.61) = 7.52 m
Required sealing pressure Ps ≈ 0.5 MPa
F=Ps × A = 0.5×(7.52×0.005)=18.8 kN
Clamping bolts and hinges are selected to deliver **> 20 kN** force uniformly.

VI. MODELLING

1. Vacuum Chamber Design

The chamber, measuring 1270 mm x 680 mm x 610 mm, was modeled and analyzed using SOLIDWORKS.

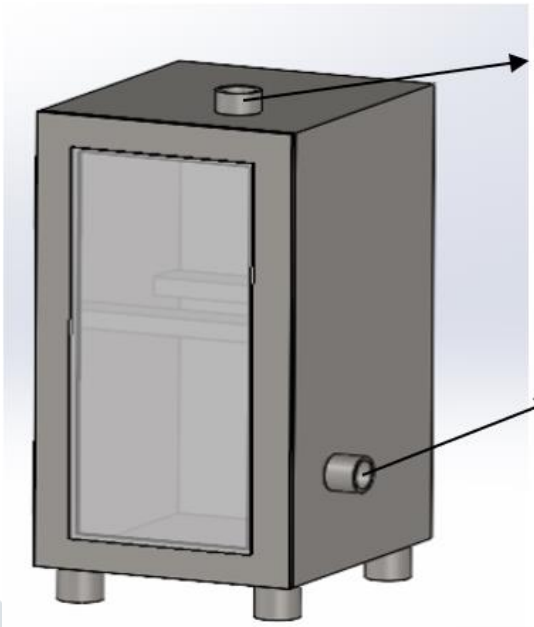

Fig 3: Vacuum Chamber

2. Die Casting Setup

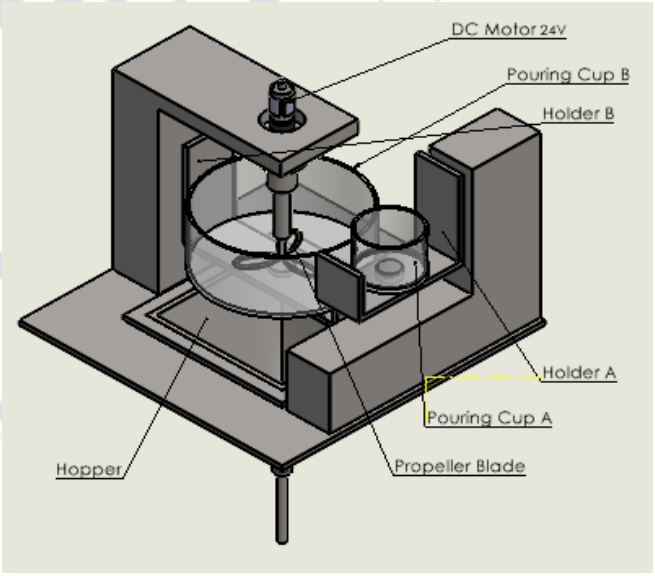

Fig 4: Die Casting Setup

At the core of the system is a 24V DC motor mounted above a transparent circular vacuum chamber, which drives a submerged propeller blade to ensure uniform mixing and eliminate material inconsistencies. Two pouring cups—Pouring Cup A and Pouring Cup B—are positioned on the top of the system, supported by Holder A and Holder B, respectively, allowing controlled addition of base material and additives or catalysts. A hopper is integrated to facilitate the safe and efficient introduction of raw materials into the system. The transparent chamber enables visual monitoring and operates under vacuum to remove air bubbles during mixing.

ISSN (Online) 2456-1290

International Journal of Engineering Research in Mechanical and Civil Engineering (IJERMCE)

Volume 12, Issue 10, October 2025

VII. ANALYSIS AND RESULTS

1. Static Structural Analysis

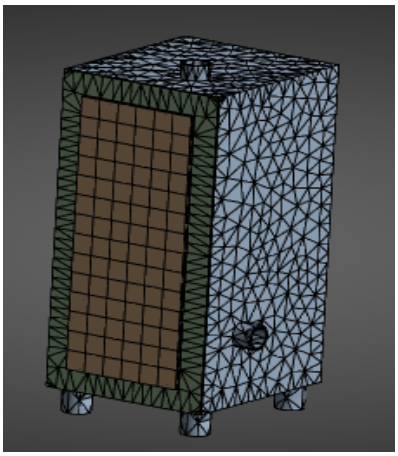

Fig 5: Mesh and Boundary Conditions

Vacuum chamber, where fixed supports are applied at the base, atmospheric pressure of **1.013e-004 GPa** is assigned to the exterior surfaces, and an internal vacuum pressure of **1.0e-006 GPa** is applied to simulate evacuation loading. This configuration replicates the real operational stress scenario during vacuum conditions. The second image presents the finite element mesh of the chamber generated using **tetrahedral elements** with localized refinement on critical regions such as the door panel and outlet port. The denser mesh on the front door ensures accurate capture of deformation and stress concentrations under the applied pressure differential, while the overall mesh maintains a balance between computational efficiency and result accuracy.

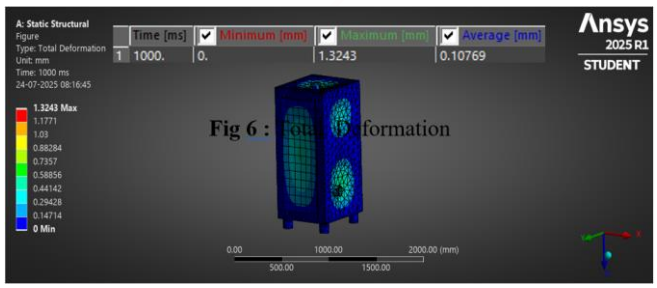

Fig 6: Total Deformation

The structural integrity of the vacuum chamber walls was verified under external atmospheric pressure conditions. The analysis confirmed that the maximum displacement occurred at the center of the side panels and remained well within acceptable limits, measuring less than **1 mm**. The Von Mises stress distribution throughout the structure was found to be below **110 MPa**, which is significantly lower than the yield strength of the material used. These results validate the chamber's ability to withstand vacuum conditions without risk of structural failure or deformation.

2. CFD Analysis

Meshing

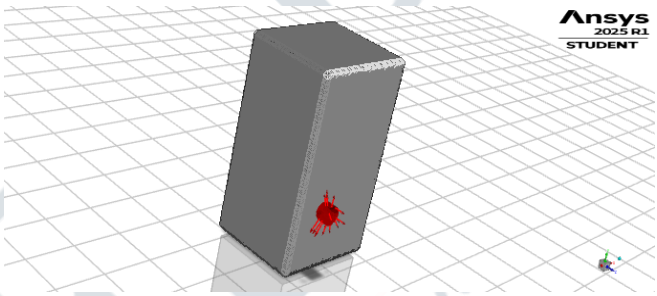

Fig 7: Meshing

The mesh was generated using hexahedral elements with an approximate element size of **5 mm**. This meshing strategy ensures a balanced trade-off between computational efficiency and solution accuracy, providing sufficient resolution to capture the structural and flow characteristics of the vacuum casting system during simulation.

Boundary Conditions

- Pressure-based, steady-state
- Laminar Flow
- Ideal gas

Initial Conditions

- Initial Pressure: **0 Pa (Gauge Pressure) = 101.325 Pa (Atmospheric Pressure)**

Outlet Conditions

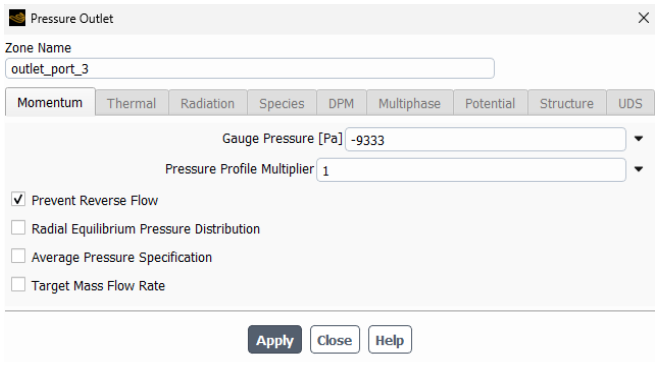

Fig 8: Pressure-outlet {0 Pa = -9333Pa (Gauge pressure)}

In ANSYS Fluent from Fig.7 the initial boundary conditions for the vacuum die casting chamber simulation

ISSN (Online) 2456-1290

International Journal of Engineering Research in Mechanical and Civil Engineering (IJERMCE)

Volume 12, Issue 10, October 2025

were defined to replicate realistic evacuation conditions and ensure accurate solution convergence. The outlet was set to a pressure outlet with a gauge pressure of **−9333 Pa** (equivalent to 70 Torr), representing the target vacuum level, while the remaining internal walls were treated as stationary, no-slip boundaries. The external environment was modeled at atmospheric pressure (101325 Pa) to establish the driving pressure differential. An initial gauge pressure of 0 Pa was applied to the chamber interior to represent pre-evacuation conditions, and air at standard density and viscosity was used as the working fluid. These boundary conditions allowed the solver to accurately capture transient pressure reduction, flow velocity distribution, and eventual steady-state vacuum maintenance within the chamber.

Simulation Results:

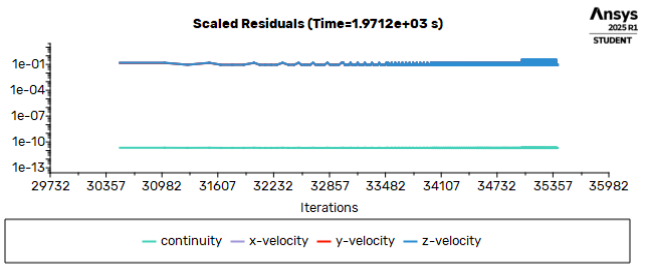

Fig 9: Scaled Residuals

The scaled residuals plot for the vacuum die casting chamber simulation, recorded at **1.9712 × 10³ seconds**, shows that continuity and all velocity components (x, y, and z) converged to very low magnitudes, with values approaching 1×10^{-10} or lower, indicating excellent numerical stability and accuracy. The residual trends remain flat after many iterations, confirming that the solution reached steady-state conditions with minimal changes in flow and pressure fields. This level of convergence ensures that the CFD results, including pressure distribution and velocity profiles, are reliable for evaluating the chamber's vacuum performance.

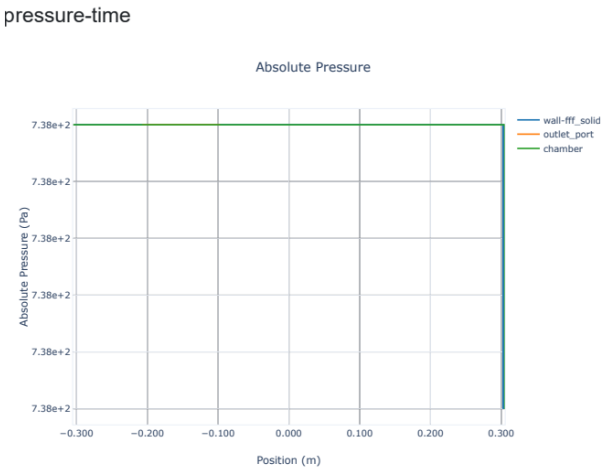

Fig 10: Pressure Plot

The pressure is consistent across the chamber, maintaining around 738 Pa(abs), which matches the target vacuum pressure and validates proper vacuum chamber design.

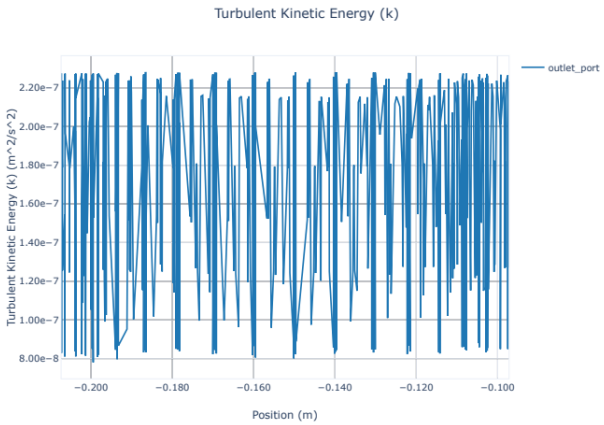

Fig 11: Turbulence KE

The TKE remains extremely low (~10^{-7} m²/s²), confirming laminar flow conditions at the outlet—ideal for controlled vacuum evacuation without turbulence.

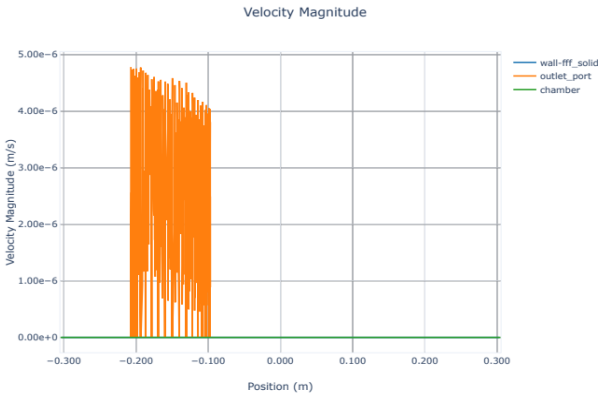

Fig 12: Mass Flow Velocity

The outlet velocity is in the micro range (~10^{-6} m/s), indicating a stable and gradual evacuation, suitable for precise casting operations without air entrapment.

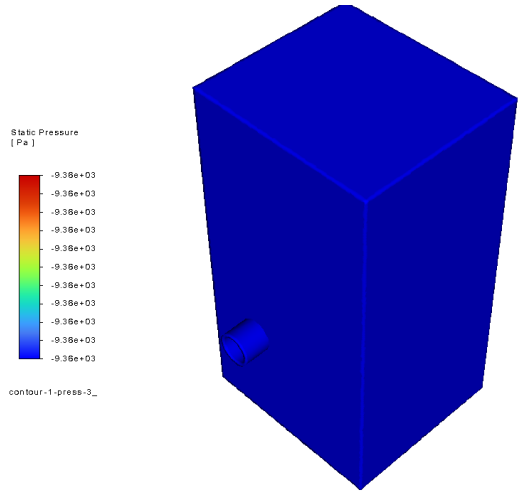

ISSN (Online) 2456-1290

International Journal of Engineering Research in Mechanical and Civil Engineering (IJERMCE)

Volume 12, Issue 10, October 2025

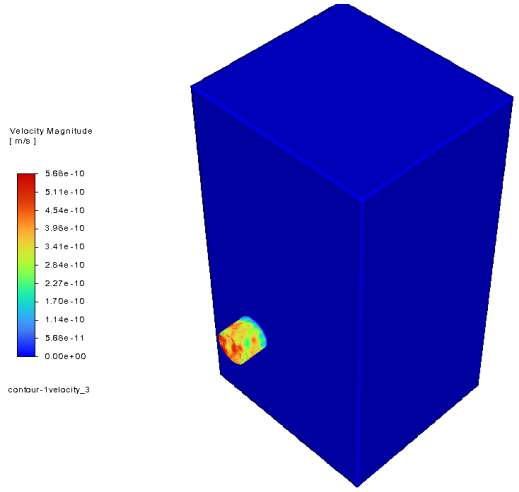

Fig 13: Pressure and Velocity Contours

The presented contour plots show the static pressure and velocity magnitude distributions from a CFD simulation of the vacuum chamber designed for the vacuum die casting system. In the static pressure plot, the internal surfaces exhibit a uniform pressure of approximately -9.36×10^3 Pa gauge, corresponding to the applied vacuum condition of 70 Torr, indicating effective depressurization across the chamber volume. The velocity magnitude plot reveals very low flow velocities (on the order of 10^{-10} m/s), concentrated primarily at the outlet port region, reflecting minimal air movement once the chamber reaches near steady-state vacuum. These results confirm the system's capability to maintain a stable low-pressure environment critical for defect-free, high-precision die casting operations.

VIII. PROTOTYPE FABRICATION

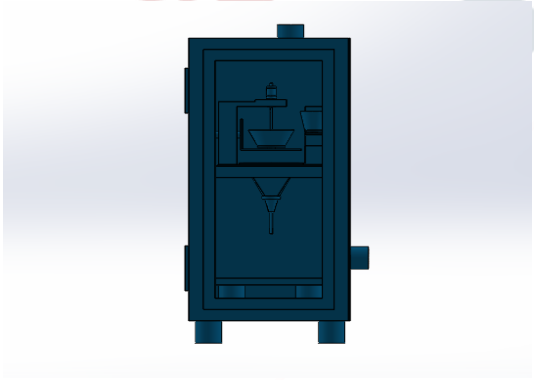

Fig 14: CAD Model for 3D Printing

To validate the physical design and assess assembly feasibility, a scaled 3D-printed prototype of the vacuum die casting system was fabricated. The CAD model was exported in STL format and processed using slicing software suitable for FDM 3D printing. PLA material was used due to its ease of printing and dimensional stability. The prototype effectively demonstrated component placement, spatial clearances, and integration of elements such as the vacuum chamber, pouring cups, and stirring mechanism, enabling early identification of potential design adjustments.

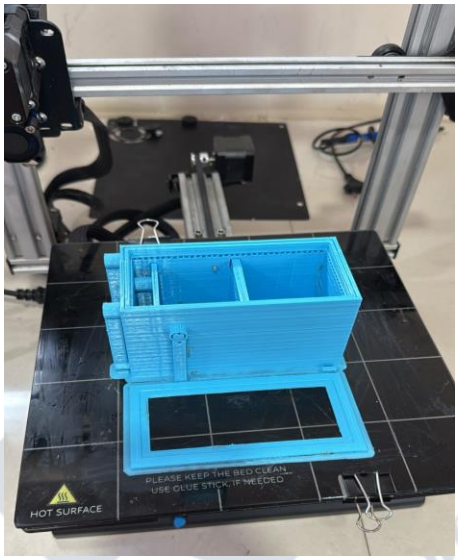

Fig 15: Prototypic Model with Support Structures

Ultimaker Cura, an open-source slicing software, played a key role in the rapid prototyping phase of this project. It was used to convert CAD models of vacuum chamber components—such as sealing profiles, observation ports, and fixture assemblies—into G-code instructions for 3D printing. Cura enabled precise control over print parameters including infill density, wall thickness, and layer height, ensuring that the prototypes maintained structural integrity and dimensional accuracy. The software also provided visual slicing previews, helping identify overhangs or unsupported geometries before printing. Using materials like PLA and PETG, various parts were prototyped to validate fitment, design ergonomics, and assembly tolerances prior to full-scale fabrication. This iterative approach reduced material waste, enhanced design confidence, and accelerated development timelines.

Fig 16: 3D Printed Prototype

A 3D printed model of the vacuum chamber was developed to visualize the design, verify dimensional accuracy, and test component assembly before final manufacturing. Printed using PLA material, the scaled prototype included key features such as the chamber door, sealing interfaces, and viewport placements. This model helped assess the spatial arrangement of valves, fittings, and observation windows, enabling early detection of design flaws. It also served as a functional demonstration tool for presenting the project concept and validating ergonomic and functional aspects of the chamber structure.

IX. CONCLUSION

The development of a high-dimensional precision vacuum die casting system for silicone and polyurethane components has been successfully achieved through a multi-disciplinary approach involving CAD modeling, CFD simulations, structural analysis, and physical prototyping. The chamber design demonstrated excellent structural integrity under vacuum loading, with minimal deformation and stress well below the material yield strength. CFD results confirmed uniform evacuation, acceptable pressure drop, and stable flow conditions, validating the vacuum efficiency critical for high-quality casting. The 3D-printed prototype further helped visualize the assembly and assess functional integration. Overall, the project proves the feasibility of a custom-engineered vacuum casting system tailored for high-precision polymer components, addressing key challenges in material handling, air entrapment, and mold filling efficiency.

X. FUTURE SCOPE

For further enhancement of the system, future work can focus on integrating thermal analysis to evaluate heat transfer during the casting process, particularly for temperature-sensitive materials like silicone and polyurethane. Real-time pressure and temperature sensors can be embedded to enable automated monitoring and control for better process consistency. Advanced material studies, including compatibility testing with various mold coatings and release agents, are recommended to improve surface finish and reduce post-processing. Additionally, scaling the system for industrial applications and incorporating a fully automated pouring mechanism can improve efficiency. Experimental validation through actual casting trials will also help correlate simulation data with practical outcomes, ensuring robustness and reliability of the design.

REFERENCES

[1] X. Chen, Y. Huang, and B. Wu, “Advanced materials for precision vacuum die casting moulds,” *J. Mater. Process. Technol.*, vol. 329, pp. 117088, Jan. 2024.

[2] C. García, J. Lopez, and M. Alvarez, “Smart sensor integration in vacuum die casting,” *Sensors*, vol. 23, no. 4, pp. 1884, Feb. 2023.

[3] L. Wang, K. Chen, and Y. Zhou, “Machine learning-based control of industrial vacuum systems,” *IEEE Trans. Ind. Informatics*, vol. 18, no. 9, pp. 6123–6132, Sept. 2022.

[4] K. Ito and S. Nakamura, “AI-based predictive maintenance of vacuum systems,” *IEEE Trans. Autom. Sci. Eng.*, vol. 19, no. 2, pp. 1193–1204, 2022.

[5] E. Martínez and D. Ruiz, “Smart vacuum systems with IoT integration,” *IEEE Internet Things J.*, vol. 9, no. 4, pp. 2871–2882, Feb. 2022.

[6] C. Nguyen et al., “Deep learning for vacuum leakage detection,” *IEEE Trans. Ind. Electron.*, vol. 69, no. 11, pp. 11630–11640, Nov. 2022.

[7] K. Sato and J. Tanaka, “Smart vacuum die casting with adaptive control,” *J. Manuf. Syst.*, vol. 62, pp. 136–145, 2022.

[8] R. Mohan and S. Nair, “Leak detection and mitigation in vacuum chambers,” *Vacuum*, vol. 198, pp. 110789, 2022.

[9] G. Liu and Y. Wang, “Advanced materials for high-precision die casting,” *Mater. Today Commun.*, vol. 30, pp. 103087, 2022.

[10] A. Patel and R. Singh, “CFD analysis of evacuation dynamics in vacuum die casting,” *Mater. Today Proc.*, vol. 44, pp. 2123–2130, Dec. 2021.

[11] S. Lee and H. Kim, “Leakage control in high-precision vacuum systems,” *Vacuum*, vol. 194, pp. 110324, 2021.

[12] M. Kumar and V. Sharma, “Thermal analysis of vacuum chambers using CFD,” *Heat Transf. Eng.*, vol. 42, no. 10, pp. 843–852, 2021.

[13] L. Zhao et al., “Hybrid vacuum pumps for energy efficiency in casting,” *Energy Rep.*, vol. 7, pp. 1516–1524, Nov. 2021.

[14] Y. Zhang, “Transient evacuation simulations in vacuum casting,” *J. Manuf. Process.*, vol. 61, pp. 167–175, 2021.

[15] N. Patel and M. Desai, “Effect of chamber geometry on evacuation performance,” *Int. J. Thermofluids*, vol. 12, pp. 100096, 2021.

[16] J. Luo, H. Zhou, and X. Li, “Design of Industry 4.0 vacuum casting systems,” *Procedia CIRP*, vol. 99, pp. 309–314, 2021.

[17] K. Tanaka, “High-speed evacuation modeling using CFD,” *Vacuum*, vol. 195, pp. 110448, 2021.

[18] R. Patel, “Robust sealing design for vacuum chambers,” *J. Mater. Process. Technol.*, vol. 291, pp. 117041, 2021.

[19] F. Rossi and G. Bianchi, “CFD simulation of evacuation performance,” *Comput. Fluids*, vol. 223, pp. 104955, 2021.

[20] D. Nguyen and A. Pham, “Advanced automation in vacuum die casting,” *Procedia CIRP*, vol. 98, pp. 476–481, 2021.

[21] J. Li and M. Zhao, “Pressure transient modeling for vacuum systems,” *Chem. Eng. Sci.*, vol. 241, pp. 116745, 2021.

[22] P. Zhou, “Enhanced evacuation modeling using turbulence models,” *Int. J. Thermofluids*, vol. 12, pp. 100122, 2021.

[23] V. Garg and P. Mehta, “Effect of surface roughness on leakage rates,” *Mater. Des.*, vol. 200, pp. 109426, 2021.

[24] R. Kumar and T. Jain, “Vacuum chamber heat transfer modeling,” *Int. J. Heat Mass Transf.*, vol. 172, pp. 121144, 2021.

[25] L. Rossi and E. Conti, “Simulation-based design of vacuum systems,” *Comput. Aided Des.*, vol. 138, pp. 103037, 2021.

[26] D. Zhao, “AI algorithms for evacuation optimization,” *IEEE Access*, vol. 9, pp. 112345–112356, 2021.

[27] N. Chandra and S. Patel, “Real-time vacuum monitoring with smart sensors,” *IEEE Sensors J.*, vol. 21, no. 19, pp. 22146–22155, Oct. 2021.

[28] S. Banerjee and R. Sharma, "Material flow analysis in vacuum die casting," *Mater. Today Commun.*, vol. 26, pp. 102039, 2021.
[29] M. Verma et al., "Multi-objective optimization of die casting cycles," *Appl. Soft Comput.*, vol. 103, pp. 107155, 2021.
[30] F. Ahmed, "Digital twin modeling for vacuum casting," *Comput. Ind.*, vol. 132, pp. 103501, 2021.
[31] B. Wang and Y. Chen, "Real-time monitoring in vacuum die casting," *IEEE Access*, vol. 8, pp. 128543–128551, 2020.
[32] M. Thomas, "Vacuum pressure profiles and simulation validation," *J. Vac. Sci. Technol. B*, vol. 38, no. 4, pp. 042201, 2020.